A Simple Technique for Propagation Characteristics of Substrate Integrated Waveguide

Esfandiar Mehrshahi and Mehdi Salehi

Department of Electrical and Computer Engineering
Shahid Beheshti University, G. C., Tehran, Iran
mehr@cc.sbu.ac.ir, m_salehi@sbu.ac.ir

Abstract ─ A simple technique is presented for propagation characteristics of substrate integrated waveguide (SIW). A unit cell of the periodic structure is divided into consecutive rectangular waveguide sections with small difference in widths. Each section is modeled by a transfer matrix which is calculated by satisfying the boundary conditions on discontinuities. Propagation constant of the SIW is extracted by applying the Floquet theorem to the overall transfer matrix of a single unit cell. The results of this extremely simple method agree well with measured values and other numerical techniques reported in recent literatures.

Index Terms ─ Dispersion characteristic, periodic structure, substrate integrated waveguide (SIW), transfer matrix, waveguide discontinuity.

I. INTRODUCTION

To a great extent, systems are based on planar structures which often exhibit high losses. On the other hand, non-planar metallic waveguides are low-loss structures with high power handling capability. The substrate integrated waveguide (SIW) is a periodic structure which preserves well-known advantages of both conventional rectangular waveguide and microstrip transmission line. Hence, SIW is a promising structure for microwave planar circuits such as filters, resonators, mixers, and antennas [1-4]. Various analytical and numerical techniques, namely, the finite-difference frequency-domain (FDFD), the method of lines (MoL), and the boundary integral-resonant mode expansion (BI-RME) method have been employed to analyze SIW structures [5-7]. However, most of them are time and memory consuming and rarely give physical insight about the performance of the structure. Also, risk of divergence solutions may exist; these methods can be very accurate and efficient.

Based on the above observations, this raises the motivation in devising an efficient method to meet the challenges for accuracy, simulation time, required memory, and complexity. In this paper, a very simple approach is proposed to approximately calculate SIW characteristics. The reported results indicate that the electromagnetic field intensity radiated out of two rows of holes is negligible under condition of $\frac{S}{d} \le \frac{5}{2}$ [8] where S and d are longitudinal spacing and diameter of metal vias in the SIW structure, respectively. Hence, the area between adjacent via holes can be modeled by the electric wall. This concept allows for approximating the structure by consecutive rectangular waveguide sections with slightly different widths. By applying the Floquet theorem to overall transfer matrix of a single unit cell, the dispersion properties of the structure are obtained.

The paper is organized as follows. In section II, the overall transfer matrix of a single unit cell is calculated by approximating the configuration with consecutive waveguide steps. Simulation results compared with numerical and experimental values are presented in section III. Finally, section IV concludes the paper.

II. DESCRIPTION OF THE METHOD

The geometry of the SIW structure with its physical parameters is shown in Fig. 1. A period of the structure, indicated in Fig. 2(a), can be approximated by cascading of rectangular waveguide sections with slightly different widths. It is well-known that the selected unit cell is not the unique choice and another periodic structure can be obtained by shifting the configuration to the

1054-4887 © 2010 ACES

left/right by a distance of, for example, *S/2*. On the other hand, the starting point of the unit cell doesn't affect the final results.

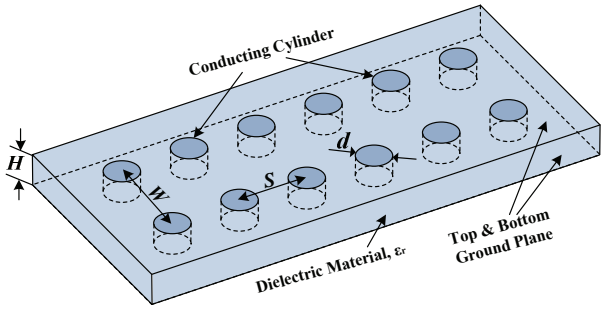

Fig. 1. 3D view of the SIW.

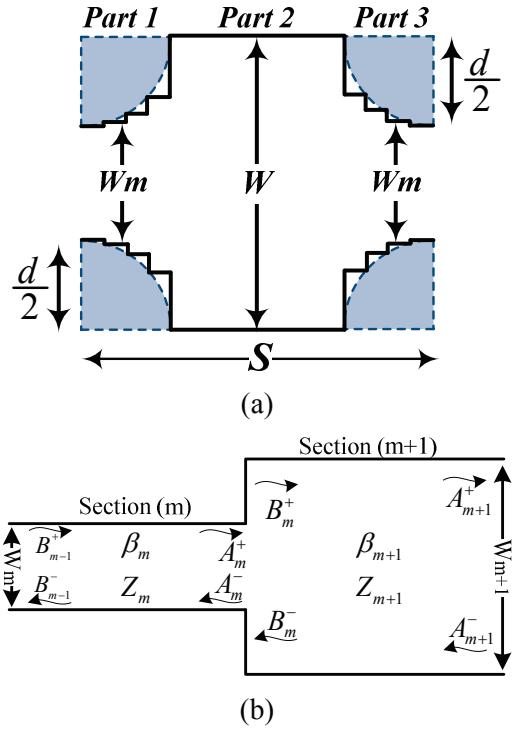

Fig. 2. Top view of the SIW structure: (a) a single unit cell and (b) m^{th} discontinuity.

The unit cell of the whole SIW, as shown in Fig. 2(a), is composed of three parts. The first one consists of the quarters of two lateral cylinders that are divided into *N* consecutive waveguide sections. Each of these sections have constant length of $\frac{d}{2N}$, increasing width of W_m (for *m=1,...N*), and constant height of *H* which are denoted as section *1* to *N*. Due to the fact that pointing power toward the gaps between metal vias is rapidly evanesced, the open area out of two via holes is well approximated by using electric walls that have the shortest length and longest width. As a result, the second part includes a waveguide with length of *(S-d)*, width of $W_{N+1}=W$, and the same height. Finally, the third part consists of the quarters of two next lateral cylinders that are divided into *N* sections just the same as the first one. The discontinuity between m^{th} and $(m+1)^{th}$ sections of the first part is illustrated in Fig. 2(b). As it shows, in the left-hand side of the discontinuity, fields can be written as a summation of forward and backward TE_{10} waves for $m = 1, 2, ..., N$ as follows

$$\begin{cases} E_m^{Left} = A_m^+ cos(\frac{\pi x}{W_m}) e^{+j\beta_m z} + A_m^- cos(\frac{\pi x}{W_m}) e^{-j\beta_m z} \\ H_m^{Left} = -\frac{A_m^+}{Z_m} cos(\frac{\pi x}{W_m}) e^{+j\beta_m z} + \frac{A_m^-}{Z_m} cos(\frac{\pi x}{W_m}) e^{-j\beta_m z} \end{cases}, \quad (1)$$

and similarly in the right-hand side as

$$\begin{cases} E_m^{Right} = B_m^+ cos(\frac{\pi x}{W_{m+1}}) e^{+j\beta_{m+1} z} + B_m^- cos(\frac{\pi x}{W_{m+1}}) e^{-j\beta_{m+1} z} \\ H_m^{Right} = -\frac{B_m^+}{Z_{m+1}} cos(\frac{\pi x}{W_{m+1}}) e^{+j\beta_{m+1} z} + \frac{B_m^-}{Z_{m+1}} cos(\frac{\pi x}{W_{m+1}}) e^{-j\beta_{m+1} z} \end{cases}, \quad (2)$$

where

$$\beta_m = \sqrt{\omega^2 \mu\varepsilon - (\frac{\pi}{W_m})^2}$$

$$Z_m = \frac{\omega\mu}{\beta_m}$$

$$W_m = \begin{cases} W - d\sqrt{1-(\frac{m-1}{N})^2} & m = 1, 2, ..., N \\ W & m = N+1 \end{cases}.$$

Neglecting all loss mechanisms, by applying the boundary conditions to the electric and magnetic fields in (1) and (2), the transfer matrix of each discontinuity in the first part for $m = 1, 2, ..., N$ can be extracted as follows

$$\begin{bmatrix} B_m^+ \\ B_m^- \end{bmatrix} = \frac{Z_{m+1} W_m}{4\kappa_m} \cdot \begin{bmatrix} \frac{\lambda_m}{Z_{m+1}} + \frac{1}{Z_m} & \frac{\lambda_m}{Z_{m+1}} - \frac{1}{Z_m} \\ \frac{\lambda_m}{Z_{m+1}} - \frac{1}{Z_m} & \frac{\lambda_m}{Z_{m+1}} + \frac{1}{Z_m} \end{bmatrix} \begin{bmatrix} A_m^+ \\ A_m^- \end{bmatrix}, \quad (3)$$

where

$$\lambda_m = \frac{W_m W_{m+1}}{4\kappa_m^2}$$

$$\kappa_m = \frac{2}{\pi} \frac{W_m}{\left(1-(\frac{W_m}{W_{m+1}})^2\right)} cos(\frac{\pi}{2} \frac{W_m}{W_{m+1}}).$$

It is worth mentioning that the value of λ_m tends to 1 by increasing the number of sections and hence,

simplify transfer matrices. Similarly, the transfer matrix of each discontinuity in the third part for $m = 1, 2, ..., N$ can be extracted as follows

$$\begin{bmatrix} B_m^+ \\ B_m^- \end{bmatrix} = \frac{Z_m K_m}{W_m} \begin{bmatrix} \frac{1}{\lambda_m Z_m} + \frac{1}{Z_{m+1}} & \frac{1}{\lambda_m Z_m} - \frac{1}{Z_{m+1}} \\ \frac{1}{\lambda_m Z_m} - \frac{1}{Z_{m+1}} & \frac{1}{\lambda_m Z_m} + \frac{1}{Z_{m+1}} \end{bmatrix} \begin{bmatrix} A_m^+ \\ A_m^- \end{bmatrix}. \quad (4)$$

Delay matrix between each consecutive discontinuity in the first and third parts can be expressed as following transfer matrixes, respectively.

$$\begin{bmatrix} A_m^+ \\ A_m^- \end{bmatrix} = \begin{bmatrix} e^{-j\beta_m \frac{d}{2N}} & 0 \\ 0 & e^{+j\beta_m \frac{d}{2N}} \end{bmatrix} \begin{bmatrix} B_{(m-1)}^+ \\ B_{(m-1)}^- \end{bmatrix}, \quad (5)$$

$$\begin{bmatrix} A_{(m-1)}^+ \\ A_{(m-1)}^- \end{bmatrix} = \begin{bmatrix} e^{-j\beta_m \frac{d}{2N}} & 0 \\ 0 & e^{+j\beta_m \frac{d}{2N}} \end{bmatrix} \begin{bmatrix} B_m^+ \\ B_m^- \end{bmatrix}. \quad (6)$$

Delay matrix of the second part ($\boldsymbol{T}_{P2}$) is given by

$$\begin{bmatrix} A_N^+ \\ A_N^- \end{bmatrix} = \underbrace{\begin{bmatrix} e^{-j\beta_N (S-d)} & 0 \\ 0 & e^{+j\beta_N (S-d)} \end{bmatrix}}_{\boldsymbol{T}_{P2}} \begin{bmatrix} B_N^+ \\ B_N^- \end{bmatrix}. \quad (7)$$

At last, the overall transfer matrix of the single unit cell, using the matrices of (3), (4), (5), (6), and (7) can be written as

$$\boldsymbol{T} = \boldsymbol{T}_{P3} \boldsymbol{T}_{P2} \boldsymbol{T}_{P1}, \quad (8)$$

where $\boldsymbol{T}_{Pi}$ ($i=1,2,3$) indicates transfer matrix of the i^{th} part as given by (7) and (9).

Taking the periodicity of the structure into account, we can employ the advantage of Floquet theorem. As a result of the theorem and according to (8), propagation constant of the SIW is written as below:

$$\cosh(j\beta S) = \frac{T_{11} + T_{22}}{2},$$

where β and S are propagation constant and period length of the SIW structure, respectively.

III. SIMULATION RESULTS

The empirical equations for equivalent width of the SIW are proposed for sufficiently small S in [8-10], respectively, as follows

$$W_{eff} = W - \frac{d^2}{0.95S}, \quad (10)$$

$$W_{eff} = W - 1.08\frac{d^2}{S} + 0.1\frac{d^2}{W}, \quad (11)$$

$$W = \frac{2W_{eff}}{\pi} \cot^{-1}\left(\frac{\pi S}{4W_{eff}} Ln\left(\frac{S}{2d}\right) \right). \quad (12)$$

It is shown, in the following, that the presented technique provides good agreement with recently theoretical and experimental data, as well as equivalent width formulas in a wide range of frequency and dimension parameters.

Selecting the number of sections N, is of importance for evaluating the performance of the employed method. By choosing *N=1*, the considered unit cell is simplified to three cascaded rectangular waveguides with width of *(W-d), W,* and *(W-d)*, and hence, maximum available cut off frequency of the SIW structure is achieved compared to other values of N. In order to confirm convergence of the method, dispersion characteristic, as a function of the number of steps, is shown in Fig. 3. By increasing the number of steps, more accuracy is obtained and results are converged. However, due to the proposed model (lateral-wall approximation) and neglecting high-order mode effects, the cut off frequency slightly deviates from trusted values in [8]. On the other hand, large value of N leads to small-width discontinuities and hence, more accurate model is achieved for via holes at the cost of a small error. Based on the results, in the following examples, we consider *N=100*, which is sufficient to achieve a more accurate model for via holes and, hence, suitable accuracy.

As the first case, consider an SIW with the geometry parameters of *W=7.2 mm, d=0.8 mm S=2 mm,* and the relative permittivity ε_r*=2.33*. The

$$\boldsymbol{T}_{P1} = \left(\frac{Z_N W_{N-1}}{4K_{N-1}}\right) \begin{bmatrix} \left(\frac{\lambda_{N-1}}{Z_N} + \frac{1}{Z_{N-1}}\right) e^{-j\beta_{N-1}\frac{d}{2N}} & \left(\frac{\lambda_{N-1}}{Z_N} - \frac{1}{Z_{N-1}}\right) e^{+j\beta_{N-1}\frac{d}{2N}} \\ \left(\frac{\lambda_{N-1}}{Z_N} - \frac{1}{Z_{N-1}}\right) e^{-j\beta_{N-1}\frac{d}{2N}} & \left(\frac{\lambda_{N-1}}{Z_N} + \frac{1}{Z_{N-1}}\right) e^{+j\beta_{N-1}\frac{d}{2N}} \end{bmatrix} \ldots \left(\frac{Z_2 W_1}{4K_1}\right) \begin{bmatrix} \left(\frac{\lambda_1}{Z_2} + \frac{1}{Z_1}\right) e^{-j\beta_1\frac{d}{2N}} & \left(\frac{\lambda_1}{Z_2} - \frac{1}{Z_1}\right) e^{+j\beta_1\frac{d}{2N}} \\ \left(\frac{\lambda_1}{Z_2} - \frac{1}{Z_1}\right) e^{-j\beta_1\frac{d}{2N}} & \left(\frac{\lambda_1}{Z_2} + \frac{1}{Z_1}\right) e^{+j\beta_1\frac{d}{2N}} \end{bmatrix}$$

$$\boldsymbol{T}_{P3} = \left(\frac{Z_1 K_1}{W_1}\right) \begin{bmatrix} \left(\frac{1}{\lambda_1 Z_1} + \frac{1}{Z_2}\right) e^{-j\beta_1\frac{d}{2N}} & \left(\frac{1}{\lambda_1 Z_1} - \frac{1}{Z_2}\right) e^{-j\beta_1\frac{d}{2N}} \\ \left(\frac{1}{\lambda_1 Z_1} - \frac{1}{Z_2}\right) e^{+j\beta_1\frac{d}{2N}} & \left(\frac{1}{\lambda_1 Z_1} + \frac{1}{Z_2}\right) e^{+j\beta_1\frac{d}{2N}} \end{bmatrix} \ldots \left(\frac{Z_{N-1} K_{N-1}}{W_{N-1}}\right) \begin{bmatrix} \left(\frac{1}{\lambda_{N-1} Z_{N-1}} + \frac{1}{Z_N}\right) e^{-j\beta_{N-1}\frac{d}{2N}} & \left(\frac{1}{\lambda_{N-1} Z_{N-1}} - \frac{1}{Z_N}\right) e^{-j\beta_{N-1}\frac{d}{2N}} \\ \left(\frac{1}{\lambda_{N-1} Z_{N-1}} - \frac{1}{Z_N}\right) e^{+j\beta_{N-1}\frac{d}{2N}} & \left(\frac{1}{\lambda_{N-1} Z_{N-1}} + \frac{1}{Z_N}\right) e^{+j\beta_{N-1}\frac{d}{2N}} \end{bmatrix}. \quad (9)$$

propagation constant as a function of frequency compared with that of rectangular waveguide whose equivalent width is calculated from (10), (11), and (12) is illustrated in Fig. 4. The comparison verifies the accuracy of the proposed method. The propagation constant calculated by empirical equation in (10) and (11) is very close to experimental measurements in [8]. Hence, the cut off frequency of our method agrees well with the results of [8, 9].

The second example refers to a substrate integrated waveguide presented in [7, 11]. Its dimensions are as follows: *W=3.97 mm, d=0.635 mm, S=1.016 mm,* and $\varepsilon_r=9.9$. Results of the propagation constant are illustrated in Fig. 5. Our simulation result is well agreed with the calculated data of [7, 11] which are compared with the measurement values reported in [11].

The cut off characteristics are of importance for evaluating the performance of the SIW. For comparison, the same parameters of [9, 10] are chosen to calculate the cut off frequencies of TE_{10} mode with respect to the cylinder diameter and cylinder spacing of metallized holes as demonstrated in Fig. 6. Our simulation results show a very good agreement with those of [8]. Also, by increasing the cylinder diameter (or by decreasing the cylinder separation) the proposed method agrees well with the results of [8, 9]. Moreover, we compare our results, shown in Fig. 6, with those of [10]. However, the cut off frequency that is calculated from analytical formula of (12) is far from the others especially at small value of lateral spacing, *W*.

In this method, we express the single mode technique to improve simplicity of the analysis. In SIW structures only TE_{n0} modes (with odd value of *n*) can be excited and extracted, due to evanescent of the surface current on lateral walls and nature of the structure [8]. Therefore, single mode analysis is possible to nearly describe the propagation constant of the fundamental SIW mode. However, more accurate results can be achieved by considering high-order mode effects at the cost of complexity, computer memory and simulation time.

In spite of the variety of methods used to characterize the propagation characteristics in SIWs, high frequency structure simulator (HFSS) software, mainly relies on the finite-element (FE) method, is one of the most accurate methods for

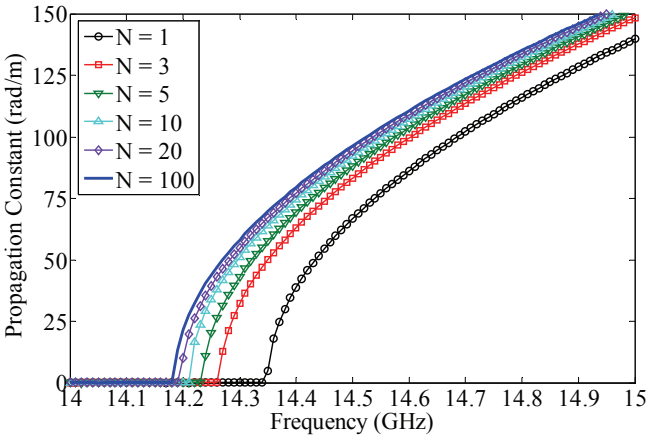

Fig. 3. Propagation constant of TE_{10} mode as a function of number of steps, *N*.

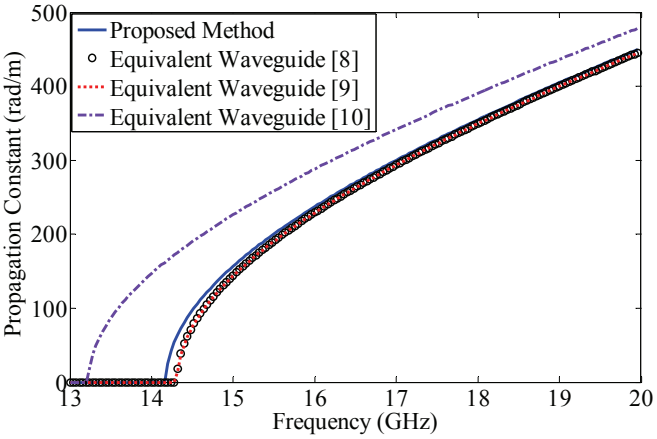

Fig. 4. Comparison of TE_{10} mode propagation constant between the proposed method and the closed-form formulas in [8-10].

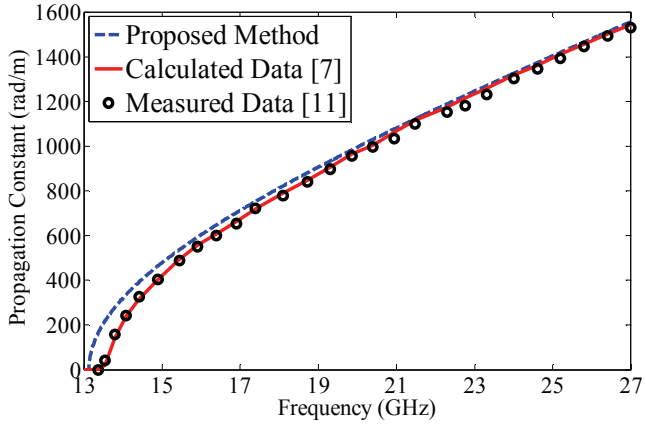

Fig. 5. Comparison of TE_{10} mode propagation constant between the proposed method and calculated results and measured data in [7, 11].

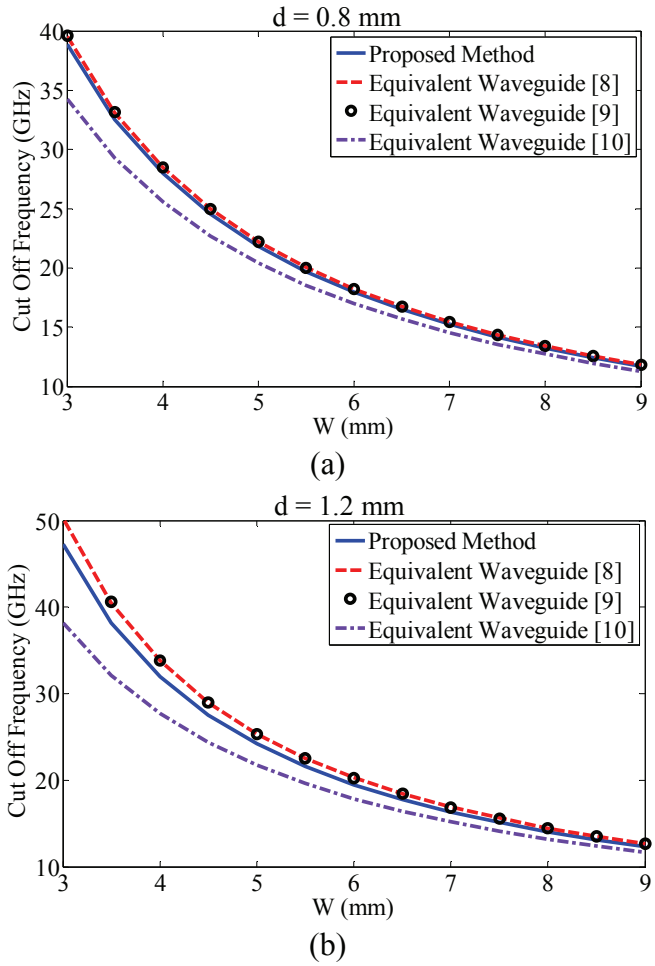

Fig. 6. Cut off frequency of TE_{10} mode with $S=1.5$ *mm* and $\varepsilon_r=2.2$ versus cylinder spacing of W and diameter of (a) $d=0.8$ *mm* and (b) $d=1.2$ *mm*.

analysis of electromagnetic problems. Hence, to demonstrate computational efficiency of the method, we make use of HFSS to solve the same problem for the comparison of the execution time, required memory, and accuracy. A single unit cell with single-mode excitation is used in HFSS to achieve propagation behavior of the SIW. Software, frequency steps, and frequency range are the same in both HFSS and proposed method. The simulation results of our method for two different numbers of sections are compared with those of HFSS and depicted in Table 1. According to the results, the typical computation time and memory requirement in the proposed technique is much less than HFSS results at the maximum cost of 0.7% error in cut off frequency.

Table 1: Execution time and required memory obtained from the proposed method and HFSS.

Methods	Time (s)	Memory (Mb)
Proposed method (N=10)	1.9	0.7
Proposed method (N=100)	5.3	4.9
HFSS + Floquet Theorem	67.1	63.1

IV. CONCLUSION

In this work, by ignoring high-order mode effects, an accurate and fast method with low memory requirements for analyzing SIW structures has been presented. The overall transfer matrix of the segmented structure is well calculated by satisfying the boundary conditions. Then, the propagation constant is calculated by applying the Floquet theorem. The significant advantage of the employed method in comparison with other numerical methods is its simplicity in computer implementation, let alone the accuracy of results. The execution time and required memory for this technique are much less than those of Ansoft's HFSS at the maximum cost of 0.7% error. The cut off frequency of TE_{10} mode with respect to the cylinder diameter d, and cylinder spacing W, is investigated to confirm accuracy of the method in a wide range of dimension parameters. The simulation results show a very good agreement with the results obtained from other numerical methods and experimental measurements over a wide frequency range.

ACKNOWLEDGMENT

The authors would like to thank Mr. Reza Rezaiesarlak for his generous cooperation in preparing the paper.

REFERENCES

[1] E. Mehrshahi, M. Salehi, and R. Rezaeisarlak, "Substrate integrated waveguide filters with stopband performance improvement," *International Conference on Microwave and Millimeter Wave Technology (ICMMT),* pp. 2018-2020, 2010.

[2] G. Angiulli, E. Arnieri, D. De Carlo *et al.*, "Fast nonlinear eigenvalues analysis of arbitrarily shaped substrate integrated waveguide (SIW) resonators," *IEEE*

Transactions on Magnetics, vol. 45, no. 3, pp. 1412-1415, 2009.

[3] C. Ji-Xin, H. Wei, H. Zhang-Cheng *et al.*, "Development of a low cost microwave mixer using a broad-band substrate integrated waveguide (SIW) coupler," *Microwave and Wireless Components Letters, IEEE,* vol. 16, no. 2, pp. 84-86, 2006.

[4] L. Bing, H. Wei, K. Zhenqi *et al.*, "Substrate integrated waveguide (SIW) monopulse slot antenna array," *IEEE Transactions on Antennas and Propagation,* vol. 57, no. 1, pp. 275-279, 2009.

[5] X. Feng, Z. Yulin, H. Wei *et al.*, "Finite-difference frequency-domain algorithm for modeling guided-wave properties of substrate integrated waveguide," *IEEE Transactions on Microwave Theory and Techniques,* vol. 51, no. 11, pp. 2221-2227, 2003.

[6] L. Yan, W. Hong, K. Wu *et al.*, "Investigations on the propagation characteristics of the substrate integrated waveguide based on the method of lines," *Microwaves, Antennas and Propagation, IEE Proceedings,* vol. 152, no. 1, pp. 35-42, 2005.

[7] M. Bozzi, L. Perregrini, and W. Ke, "Modeling of conductor, dielectric, and radiation losses in substrate integrated waveguide by the boundary integral-resonant mode expansion method," *Microwave Theory and Techniques, IEEE Transactions on,* vol. 56, no. 12, pp. 3153-3161, 2008.

[8] X. Feng and W. Ke, "Guided-wave and leakage characteristics of substrate integrated waveguide," *IEEE Transactions on Microwave Theory and Techniques,* vol. 53, no. 1, pp. 66-73, 2005.

[9] Y. Cassivi, L. Perregrini, P. Arcioni *et al.*, "Dispersion characteristics of substrate integrated rectangular waveguide," *Microwave and Wireless Components Letters, IEEE,* vol. 12, no. 9, pp. 333-335, 2002.

[10] W. Che, K. Deng, D. Wang *et al.*, "Analytical equivalence between substrate-integrated waveguide and rectangular waveguide," *Microwaves, Antennas & Propagation, IET,* vol. 2, no. 1, pp. 35-41, 2008.

[11] D. Deslandes and W. Ke, "Accurate modeling, wave mechanisms, and design considerations of a substrate integrated waveguide," *IEEE Transactions on Microwave Theory and Techniques,* vol. 54, no. 6, pp. 2516-2526, 2006.

Esfandiar Mehrshahi was born in Tehran, Iran, in 1963. He received the B.Sc. degree from the Iran University of Science and Technology, Tehran, Iran, in 1987, and the M.Sc. and Ph.D. degrees from the Sharif University of Technology, Tehran, Iran, in 1991 and 1998, respectively, all in electrical engineering. Since 1990, he has been involved in several research and engineering projects at the Iran Telecommunications Research Center (ITRC). He is currently an Assistant Professor at Shahid Beheshti University, Tehran, Iran. His main areas of interest are the nonlinear simulation of microwave circuits and low phase noise oscillators.

Mehdi Salehi was born in Isfahan, Iran, in 1979. He received the B.Sc. and M.Sc. degrees both in electrical engineering from Isfahan University of Technology (IUT), Isfahan, Iran, in 2001 and 2006, respectively. He is currently working toward his Ph.D. degree in electrical engineering at Shahid Beheshti University (SBU), Tehran, Iran. He worked as a researcher in Information and Communication Technology Institute (ICTI) on RF circuit design from 2001 to 2003. His current research interests include numerical methods in electromagnetic and advanced microwave and millimeter-wave circuits and components.